A Model for Drying Control Co-Solvent Selection for Spin Coating Uniformity: The Thin Film Limit

A Model for Drying Control Co-Solvent Selection for Spin Coating Uniformity: The Thin Film Limit

Dunbar P. Birnie, III[#]

Department of Materials Science and Engineering
Rutgers University
Piscataway, NJ 08854-8065

ABSTRACT

Striation defects in spin-coated thin films are a result of unfavorable capillary forces that develop due to the physical processes commonly involved in the spin-coating technique. Solvent evaporation during spinning causes slight compositional changes in the coating during drying, and these changes lead to instability in the surface tension and this causes lateral motions of the drying fluid up to the point where it gels and freezes-in the thickness variations. In an earlier publication we looked at the case where evaporation happens fast enough that the compositional depletion is mostly a surface effect. In terms of the mass transport rate competition within the coating solution then that work covered the thick-film limit of this instability problem. However, in many cases the coatings are thin enough or diffusion of solvent within the coating is fast enough to require a different solvent mixing strategy, which is developed here. A simple perturbation analysis of surface roughness is developed and evaporation is allowed in the thin film limit. The perturbation analysis allows for a simple rubric to be laid out for co-solvent additions that can reduce the Marangoni effect during the later stages of coating deposition and drying when the thin-film limit applies.

[#] e-mail address: “dunbar.birnie@rutgers.edu”

Introduction

Striation defects in spin coating are interesting and technologically important thickness variations in the final coating that typically have relatively long wavelength (10's to 100+ microns) and are lined up as radial patterns on the substrate/wafer [1-19]. These structures have been shown to be associated with solvent evaporation and are a result of surface tension changes that happen when solvent is leaving the free surface of the coating [1, 3, 9]. These local surface tension changes can become unbalanced in neighboring locations causing the lateral fluid motion that creates these structures. This type of surface tension imbalance is a subset of processes generally known as "the Marangoni effect" [20], which has been studied extensively and applies to many important materials fabrication processes. The Marangoni effect may be driven by either thermal or composition gradients as both of these can create the local surface tension differences that are necessary for the lateral migrations that are observed. However, the specific case of striation formation has been definitively tied to *composition*-driven Marangoni forces [10].

The modern work on striations builds from the earliest observation of convective instability in fluids heated from below, structures now commonly known as "Bénard cells" [21]. These were explained as being driven by buoyancy effects due to thermal expansion of the fluid [22, 23]. Later work found that there were also many conditions of cellular convection which were driven by surface tension [24] and other work has been done to further understand the stability criteria for these processes [25]. The importance of surface tension in convection instability has led to continuing studies where surfactants have been added to the models or more general composition variations are modeled within the fluid including composition-dependent fluid density effects [26, 27]. Thus, there are many configurations where buoyancy and surface tension effect combine or compete to create complicated roughness patterns in fluid layers.

As noted above, thickness variations in coatings made by spin-coating have been frequently observed and mostly are characterized by generally sinusoidal patterns. However, in extreme cases it has been found that thickness variations can reach a point of destabilization where pinhole formation and dewetting occurs [28-30]. But, the early development of roughness in these cases can also be explained as smaller sine-wave-like bumps.

The addition of surfactants is an important compositional strategy for reducing striations and other coating defects [31-33]. And, this idea has been extended to the practical addition of co-solvents that can change the surface tension dynamically during the spin coating and drying process[9], though only the thick film limiting case has been developed to this point (as discussed further below).

The understanding of the coating flows and striation instabilities has also been harnessed by various workers who have used the striations as waveguides [34] or as regions where suspended particles get grouped or patterned during deposition [35], or even to guide patterns of dewetted pinholes [36].

The many cases of striations in spin coating fall into the class of vigorously studied problems identifiable as “long-wavelength” instabilities [37-42] in that the fluid thickness is much smaller than the typical characteristic lateral wavelengths observed in the coatings. This distinction is very important because the Marangoni forces seldom have time to develop into full circulation patterns, but rather cause slight lateral fluid motions that end up being frozen in place when solvent evaporation progresses and the coating becomes too viscous to flow any further.

The present paper looks at the thin film limiting case of the long-wavelength instability by developing a perturbation analysis and examining conditions where evaporation will cause roughening as drying progresses. With this understanding of how perturbations will behave, a

co-solvent selection strategy is then provided that can help formulate a coating solution to reduce the coating's susceptibility to striation formation when in the thin film limit. As a starting point for this analysis, the *thick* film case is discussed so that the key differences between thick and thin film cases can be distinguished.

Background: The Thick Film Limit

In earlier work we examined the thick film limit of the evaporation-driven instability and developed a solvent selection strategy that combined features of solvent volatility and solvent surface tension values in a deliberate way [9]. Figure 1 gives the conceptual situation where a coating solution is drying on a rigid substrate in the thick film limit. Solvent evaporation happens from the top surface and is fast enough to outpace solvent diffusion within the coating solution. This results in solvent depletion from the surface that may reach a point where a skin forms (though this is not necessarily required). Physical evidence for skin formation during spin coating has been found before [43-46] and is probably quite common for coating solutions that start with higher polymer or solids content.

Through random fluctuations in local composition and evaporation then adjacent nearby regions can develop slightly different surface tension values. These surface tension *differences* lead to lateral migration of fluid toward regions with higher surface tension. As these motions happen then the flow field also stretches the thinner areas so that their skin becomes thinner and compresses the thicker areas so that their skin gets relatively thicker with time. This amplifies the evaporation-driven composition difference at the surface and causes further growth of the perturbation. Aspects of this Marangoni instability have been modeled in various limiting cases as noted above.

Our earlier work on this topic then provided a solvent-mixing strategy that would allow for staged co-solvent removal that would leave skin compositions with the opposite surface tension imbalance, with the intended effect that slight composition differences would lead to tractions aimed at *smoothing* the surface rather than allowing roughening [9]. In later work, we demonstrated this solvent mixing strategy with an Al-Ti-based sol-gel composition [11], and measured surface tension values for related solutions associated with these instabilities [47]. However, all of this work was aimed at reducing striations for the thick film limit only, and in some cases where we have tried to apply that strategy, we have found that various coating solutions did not behave as predicted in that model. Thus, in the next section we look at the thin film limit to understand what differences in drying behavior might be applicable to thinner layers, and ultimately what kind of solvent mixing strategy might be required when trying to reduce striation defects in this opposite case.

The Thin Film Limit

Figure 2 illustrates the new limiting case (opposite of the previous case). Again there is evaporation of the solvent into the ambient, but the rate of this evaporation is slow relative to the rate of diffusion of solvent in the coating solution. Also, we assume that the lateral spacing is so large that each location is essentially independent of its neighbor. So, contrary to the prior case, the coating solution remains locally relatively homogeneous, but still susceptible to an instability in a different way: If a slight thickness variation occurs as a result of natural random fluctuations then the two neighboring locations can have physically different amounts of solvent present simply because of that geometric height difference. Then, because solvent evaporation is a relatively uniform process then *the thinner regions change composition faster*. This can become

unstable if the slightly thicker areas develop higher surface tension values because of their local composition. This can lead to lateral Marangoni-effect-driven fluid migration. In this case it can once again be unstable because as the high spots contract their relative height compared to their neighbors is amplified leading to a greater difference in their drying rates. This limiting case is analyzed rigorously in the following two sections. First, the basic long-wavelength Marangoni instability analysis is developed based on a sinusoidal perturbation of an arbitrary wavelength in either height and/or surface tension. Then, the progression of such sinusoidal perturbations subject to the evaporation process shown in Figure 2 is developed and applied. These equations then provide a quantitative basis for suggesting co-solvent additions in this new thin-film limiting case.

Perturbation Analysis of Thin Film Stability with Marangoni Forces

We can see from Figures 1 and 2 that the coating is mostly flat but has a slight sinusoidal perturbation in height and/or surface tension. And, as noted in the introduction, the wavelength of striations that are typically observed are typically between one and two orders of magnitude larger than the average coating thickness. So, we can follow a simple long wavelength perturbation analysis similar to many that have been presented in the past for various different thermal and compositional boundary conditions as noted above. We treat a constant viscosity fluid subject to laminar flow governed by the Navier-Stokes equations [48].

As a starting point we model an arbitrary, small amplitude, sinusoidal thickness variation, where H_o is the average fluid depth and A is the amplitude of the physical height perturbation:

$$H(x) = H_o + A\sin(kx) \qquad (1)$$

where k is the perturbation wavenumber and x is the lateral position variable. Similarly, the surface tension can have a slight perturbation, B, around its nominal average value (Σ_o) as:

$$\sum(x) = \Sigma_o + B\sin(kx) \qquad (2)$$

Where, again, k is the wavenumber as before. Of course the surface tension perturbation can *theoretically* have a different spacing than the physical height corrugation, but we recognize that the physical situation under analysis is one where the high spots and the low spots automatically develop these surface tension perturbation values *as a result of* the competition between solvent evaporation and solvent diffusion within the coating. Also, we pick A to be a positive number so our first high spot in the x-direction will be at x=π/2k. By association with the previous instability analyses, it is understood that our worst case situation is when the high surface tension value is also at the physical high spot. So in that sense we expect the instability to only be possible for some cases when the evaporation conditions lead to B>0 in equation (2).

Now we consider the surface tension forces applied to this layer caused by two basic effects: surface curvature (always tending toward leveling) and the Marangoni effect (where higher surface tension regions pull in against neighboring lower-surface tension regions). All of this is subject to the primary Navier-Stokes equations. Neglecting gravitational effects then we have this equation for the local pressure in the fluid as a function of position [48]:

$$\frac{\partial P}{\partial x} = -\frac{\partial}{\partial x}\left[\Sigma(x)\frac{\frac{\partial^2 H(x)}{\partial x^2}}{\left[1+\left(\frac{\partial H(x)}{\partial x}\right)^2\right]^{3/2}}\right] \qquad (3)$$

By keeping Σ(x) inside the brackets then we account for the lateral surface tension variations simultaneously with the curvature effects. And, this traction variation in the x-direction causes viscous flow laterally depending on the viscosity. The lateral flow velocity will depend on height

above the substrate and the viscous forces will exactly offset the pressure developed by the surface curvature:

$$\frac{\partial P}{\partial x} = \eta \frac{\partial^2 v_x}{\partial z^2} \qquad (4)$$

The vertical velocity field is subject to the no-slip condition at the substrate surface and when integrated from substrate to surface is responsible for lateral material migration that is the core of the Marangoni effect. Lateral motion of matter then leads to growth or shrinkage of any perturbation that exists – and will depend on both H(x) and Σ(x). Performing this integration we find this expression for the change in H with time:

$$\frac{\partial H}{\partial t} = -\frac{1}{3\eta}\frac{\partial}{\partial x}\left[H^3 \frac{\partial}{\partial x}\left[\Sigma \frac{\frac{\partial^2 H}{\partial x^2}}{\left[1+\left(\frac{\partial H}{\partial x}\right)^2\right]^{3/2}}\right]\right] - \frac{1}{2\eta}\frac{\partial}{\partial x}\left[H^2 \frac{\partial \Sigma}{\partial x}\right] \qquad (5)$$

Using the sinusoidal functions for H and Σ presented as equations (1) and (2) above it is possible to expand equation (5) in full generality. But, given that we are interested in the amplification of our coating perturbation with time then we focus attention on the height change (∂H/∂t) *evaluated at the peak* of the sinusoidal perturbation (x=π/2k). For that location we associate height growth (or shrinkage) with the change in amplitude A of the H(x) function with time. And, for that location then both the first and third partial derivatives with respect to x of both H and Σ evaluate to zero at that location, and all the sine terms evaluate as either positive or negative one. After substituting the various differentials and collecting terms we get this compressed expression for ∂H/∂t evaluated at x=π/2k:

$$\frac{\partial H}{\partial t}\left(@x = \frac{\pi}{2k}\right) = -\frac{1}{3\eta} A H_o^3 [B + \Sigma_o] k^4 + \frac{1}{2\eta} B H_o^2 k^2 \qquad (6)$$

And, while there might be slight differences at the trough, we use this to represent the growth rate of the thickness perturbation which is also the rate of growth of A.

Using equation (6) it is possible to determine the wavenumber of the perturbations which will be amplified (i.e. $\partial A/\partial t>0$) and which perturbations which will be damped ($\partial A/\partial t<0$) as a result of the competing curvature and Marangoni processes. The limit of stability – or the boundary between stable and unstable – will be found by setting equation (6) to zero and solving. This results in the following expression:

$$k^2_{stability} = \frac{3B}{2AH_o\Sigma_o} \qquad (7)$$

We can see that if k^2 is greater than this value then the 4-th power term in equation (6) will dominate and the coating will get flatter with time. On the other hand for smaller values of k^2 then amplification will occur. This stability criterion puts the leveling effects of surface curvature (driven by larger A) in direct opposition to the roughening tendency of the Marangoni effect (driven by larger B).

If a wide range of perturbation frequencies are present in the system then we might expect the periodicity of the striation spacing would be most closely connected with the thickening rate that is maximal. This can be determined by differentiating equation (6) by k^2 and solving for zero. We find the periodicity of maximum amplification will be:

$$k^2_{max} = \frac{3B}{4AH_o\Sigma_o} \qquad (8)$$

This is interesting because spin coating experiments are known to show relatively homogeneous wavelength for the thickness variation pattern even comparing the center of the wafer with areas near the periphery [6].

This perturbation analysis makes no assumptions about evaporation rate or drying as it might influence the H and Σ parameters, so these features need to be addressed and combined with this stability analysis.

Evaporation Model Applied to Thin Film Coating Drying

Spin coating is a process where outward fluid flow is combined with solvent evaporation that together usually results in quite uniform coatings on a global level. Meyerhofer gave the first mathematical treatment [49], which built upon the basic fluid flow-only analysis made earlier by Emslie, Bonner, and Peck [50]. Meyerhofer added solvent evaporation to arrive at a basic equation for fluid thickness evolution as:

$$\frac{\partial H}{\partial t} = -\frac{2\rho\omega^2}{3\eta}H^3 - e \qquad (9)$$

Where H is the instantaneous fluid height, ρ is the fluid density, ω is the rotation rate, η is the fluid's viscosity, and e is the evaporation rate of the solvent. It is notable that because of the H^3 dependence, the flow behavior dominates at early time and the evaporation behavior dominates later in the process. The evaporation rate is usually limited by solvent vapor diffusion through a laminar air boundary layer induced by the rotation of the substrate, resulting in an evaporation rate that should be uniform across the entire wafer [51-53]. And, for moderate rotation speeds the evaporation rate will vary as the square root of ω. This model of combined flow and (uniform) evaporation has been verified by several groups using interferometric thinning measurements [43, 54-57] including the determination of evaporation coefficients for several volatile solvents in typical spinning configurations.

Interestingly, laser diffraction measurements showed that striations formed at about the same time that evaporation was starting to become important in the thinning equation [8]. Since that coincided with the time when equation (9) is effectively starting to be dominated by the second term, then it is reasonable to examine the Marangoni thinning based only on evaporation effects alone. This is especially true for situations that will be covered by the thin film limit: they are more dilute, aiming for thinner final coating thickness, and less likely to form a skin. Further,

it is known that striations are ridges that run radially outward from the center of the wafer [4-6, 13], whereas the sinusoidal variation direction is in the direction of rotation: so the fluid flow field is perpendicular to the Marangoni amplification process. Thus, in both regards it is reasonable to consider only evaporation effects in the ensuing analysis.

Although Meyerhofer and others considered evaporation to be uniform across the wafer, they didn't consider any local compositional variation within the coating itself from which the evaporation is taking place. Here we apply the physical insight that evaporation happens by diffusion of vapor through a boundary layer to non-solvent-containing free airflow beyond. But, we also acknowledge that the coating can have lateral composition variation (the source of the surface tension modulation) and that this will also influence the local evaporation rate.

Referring back to the surface tension modulation (equation (2) above) we know that this must be a result of composition variation. For practical linear analysis of the drying and surface tension behavior we estimate that the surface tension can be approximated according to:

$$\Sigma = \Sigma_{pure} + mC_p \qquad (10)$$

where C_p is the fractional polymer concentration of the solution, Σ_{pure} is the surface tension of the pure solvent, and **m** is the slope of the surface tension with polymer concentration (which could be negative or positive, depending on the system). With the lateral variation in surface tension then we must have this variation in $C_p(x)$:

$$C_p(x) = C_p^o + C\sin(kx) \qquad (11)$$

where, again, the composition modulation is keyed-in to the same periodicity as the height and surface tension modulations. If we consider a simple coating solution with a quantity of solvent (S) and of polymer (P) that together combine to the local thickness, H(x) = P+S, then:

$$C_p(x) = \frac{P}{P+S} \qquad (12)$$

Therefore, as only the solvent is evaporating, it leaves behind a thinner layer with gradually larger concentration of polymer as time progresses. As commented above, we apply an ideal solution model for the solvent/polymer mixture, giving that the evaporation will be tied to the local composition:

$$E(x) = e_o(1 - C_p(x)) \tag{13}$$

where e_o is the evaporation rate expected from pure solvent under the same spinning conditions. And, since only the solvent is evaporating then E(x) is exactly $-\partial S/\partial t$.

Really, we are interested in evaluating the rate of change of $C_p(x)$ with time and separating out the part that is simply an average drying effect from the part that manifests itself as a possible increase in composition modulation and therefore driving Marangoni tractions. Working from equation (11) we find:

$$\frac{\partial C_p(x)}{\partial t} = \frac{\partial C_p^o}{\partial t} + \frac{\partial C}{\partial t}\sin(kx) \tag{14}$$

The first term is the change in average composition with time and the second is the modulation growth or homogenization. Changes in these terms result from the change in absolute quantity of solvent, S, with time. Thus, differentiating equation (12) we get:

$$\frac{\partial C_p(x)}{\partial t} = \frac{e_o}{H(x)} C_p(x)\big(1 - C_p(x)\big) \tag{15}$$

Then, as we are working with small amplitude perturbations and testing the susceptibility to amplification, we can approximate equation (15) as:

$$\frac{\partial C_p(x)}{\partial t} \cong \frac{e_o C_p^o(1-C_p^o)}{H_o}\left[1 + \left[\frac{C}{C_p^o} - \frac{C}{1-C_p^o} - \frac{A}{H_o}\right]\sin(kx)\right] \tag{16}$$

Comparing equations (14) and (16) we find that the average composition will be changing as:

$$\frac{\partial C_p^o}{\partial t} \cong \frac{e_o C_p^o(1-C_p^o)}{H_o} \tag{17}$$

And that the magnitude of the composition ***modulation***, C (as defined above in equation 11), will be changing as:

$$\frac{\partial C}{\partial t} \cong \frac{e_o C_p^o (1-C_p^o)}{H_o}\left[\frac{C}{C_p^o} - \frac{C}{1-C_p^o} - \frac{A}{H_o}\right] \qquad (18)$$

We can see immediately that the A/H_o factor is always negative and tending to cause a reduction in C with time. If C is zero or already negative then it continues to become *more* negative for all experimental conditions – this is the main embodiment of the present thin film limiting case. On the other hand if C is positive then there will be some situations where C will continue to grow and some where it will become smaller, depending on the sign of the combined term in brackets.

Since we have defined C as the sinusoidal modulation in composition and have it in-phase with the roughness modulation, a positive value of C will identify a condition where the thicker areas are already a bit dryer than the thinner areas. This could occur as a result of roughness that developed earlier in the coating process (notably the thick-film limit associated with earlier times during spin coating when the fluid thickness was larger).

Solvent Selection in the Thin Film Limit

Ultimately, we are hoping to encourage processing conditions that result in flat final coatings. This would mathematically correspond to coatings with A=0 at t=∞. As with the thick film limit discussed in earlier work [9], we hope that careful solvent selection may help counteract the drying/roughening effect evidenced by equation (18). Recognizing that our ideal case will be a coating with no height fluctuation at the point when the coating is fully dry, we examine how specific solvent choices might influence the roughness growth/shrinkage. To merge the instability analysis with the drying analysis we notice that equation (2) for the surface tension used B as the amplitude of the modulation around the average value. But later, when

looking at how the composition and surface tension change as drying progresses, we have equation (10) for the composition dependence of surface tension and equation (11) for the local composition modulation. These equations will be matched only when B=mC. Knowing that the Marangoni instability will only develop when B is positive (see equation (7)), we examine conditions where the mC product will be positive. Of course, separately m and C can be either positive or negative numbers depending on the characteristics of the solvent/polymer mixture and on the rate of drying.

When the thin film limit instability limit is operating as explained in Figure 2 above then the peaks are drying slower than the troughs (this corresponds to a composition modulation in equation (11) with $C<0$). If the solvent/polymer surface tension behavior in equation (10) has $m<0$ this would leave the coating susceptible to Marangoni tractions and roughness amplification. To counteract this amplification we would like the region that is drying more slowly (the peaks) to tend toward lower surface tension relative to the average value. Since $C<0$ describes the composition modulation, and since we want the natural drying process to build a surface tension modulation that *fights* against the modulation then we would benefit from using a solvent which will give $m>0$. This means that solvents with intrinsically lower surface tension than the polymer they are dissolving would be favored to help counteract the thin-film-limit drying instability.

In a more complete view, the final coating thickness will depend on *both* the fluid thickness modulation and the composition modulation; in fact it is possible (though unlikely) for the height modulation to be exactly countered by a composition modulation of the fluid locally and still achieve a final coating that is flat. In mathematical terms we recognize that the total polymer/solids thickness after drying will be:

$$P(x) = C_p(x)H(x) = C_p^o H_o \left(1 + \frac{C}{C_p^o}\sin(kx)\right)\left(1 + \frac{A}{H_o}\sin(kx)\right) \qquad (19)$$

Because both A and C represent small perturbations around the average values then this can be approximated as

$$P(x) \cong C_p^o H_o \left(1 + (\frac{C}{C_p^o} + \frac{A}{H_o})\sin(kx)\right) \qquad (20)$$

where the prefactor product $C_p{}^oH_o$ is the expected final coating thickness if no Marangoni flow occurs. Given that A was defined as a positive number then this will require that the composition modulation have C<0 and a flat coating will result only if a specific value is maintained. However, the only practical way to achieve a flat coating is to seek conditions where lateral surface-tension-driven flows will not occur to begin with.

In this regard, if we have a polymer/solvent mixture that leaves behind striations when spin coating then it is useful to consider co-solvent additions that might counteract the coupled surface tension and drying situation that must have been operational. The first question to address is whether the coating would fit in the thick-film or thin-film limits. This can be determined by comparing the expected kinetics in the vapor phase (the evaporation rate) with the solvent diffusion rate in the solution, scaled by its depth. The dimensionless number that covers this comparison is the Sherwood number [58]:

$$Sh = \frac{eH}{D} \qquad (21)$$

where e and H are as defined before and D is the solvent diffusion rate. If Sh<<1 then diffusion is fast relative to the evaporation process and we anticipate the thin-film limit will apply. The evaporation rate in spin coating has been measured for a number of volatile solvents and depends on spin speed and solvent vapor pressure [43, 57]. For light solvents and spin speeds in the 1000-3000 range then these evaporation rates can range from ~0.1 to >10 microns per second. The

diffusion rate is tied to the viscosity through the Einstein relation, here modified according to Li and Chang [59]:

$$D = \frac{kT}{2\pi\eta}\left(\frac{N_{av}}{V}\right)^{1/3} \quad (22)$$

where, N_{av} is Avogadro's number and V is the molar volume. For light solvents then these diffusion rates will be around 10^3 $\mu m^2/s$ [60]. So, for solutions that are relatively dilute in polymer/solids content then we should fall safely within the thin film limit. For more concentrated solutions where the viscosity is larger, it is quite possible that the thick film solution will apply. The polymer-solvent interdiffusion problem and its coupling near the surface is a complicated process and can lead to skin formation as noted above, which would slow the diffusion rate substantially in that region and put it back into the thick-film situation. Thus, since the viscosity-composition relationship is often highly nonlinear, each system may yield distinctly different behaviors. A full analysis of this coupling is left for future work.

Then, the co-solvent selection issue for the thin-film limit is one of gauging the surface tension as well as the volatility and seeking to prevent the Marangoni instability during drying. If the starting coating formulation results in striations and has a relatively high-surface tension solvent then a co-solvent with full miscibility should be found such that the less volatile of the two solvents would have the higher surface tension. Then during the early part of coating drying the more volatile solvent would be extracted faster causing the remaining solution to have higher surface tension, and this effect would be more pronounced in the trough regions leading to Marangoni forces that would aid in smoothing the coating during the continued drying.

As an interesting corollary, if a researcher is interested in *enhancing* roughness rather than reducing it, then in general terms they should endeavor to select solvents in a manner contrary to the suggestions made here and in the predecessor paper [9], depending on which

regime may be applicable. Further, in many cases roughness with specific periodicity will be desired. These researchers should refer back to equation 7 above where the periodicity stability point is established. Still, once the stability point is defined, there will be a whole range of wavelengths that will be amplified, all with different rates, so the final texture may be difficult to control.

Conclusions

The present work has examined the Marangoni instability during drying for dilute solutions that will satisfy the thin film limit. A perturbation analysis shows that the gradual effect of slight thickness differences can lead to faster drying of trough regions and that these can develop surface tension imbalances that cause amplification of these perturbations. Practical drying rate parameters for real spin-coating situations are applied and the coupling between drying and local surface tension forces has been discussed. With these considerations it has been suggested that co-solvent formulations may help ameliorate this problem by providing at least a significant part of the drying with a surface tension value that increases with time and where drying rate imbalances can help reduce thickness differences.

Acknowledgements

Support from the Corning/Saint-Gobain/Malcolm G. McLaren Endowment at Rutgers University is gratefully acknowledged. Early aspects of this model were developed under NSF support through DMR 98-02334.

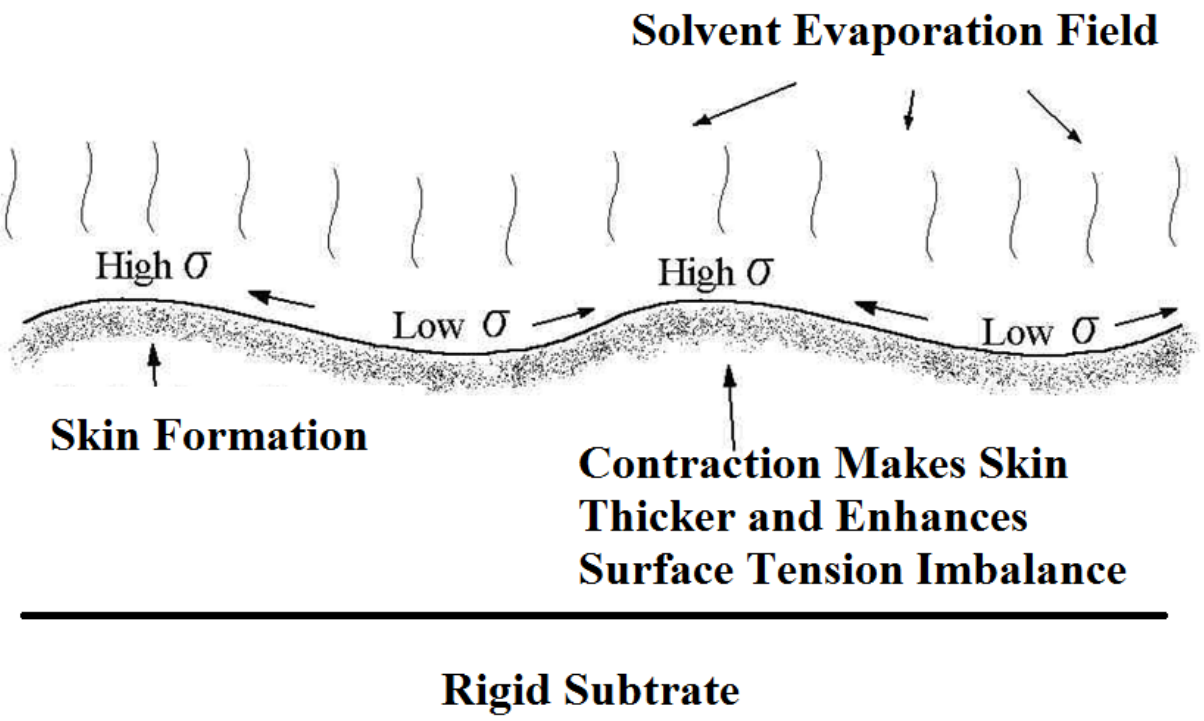

Figure 1: Schematic diagram of solvent evaporation during coating formation in the thick film limit (lateral and vertical dimensions not to scale). Solvent depletion at the surface can reach an instability point where slight surface tension imbalances lead to the Marangoni effect that amplifies with time.

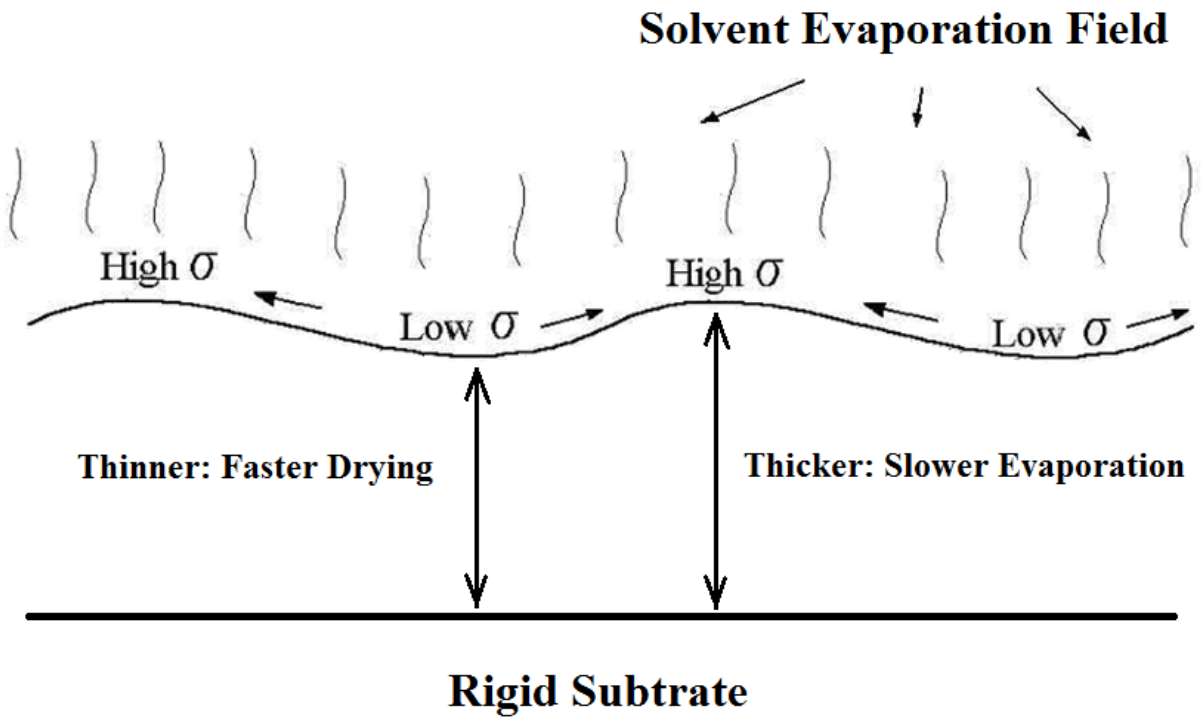

Figure 2: Schematic diagram of solvent evaporation during coating formation in the thin film limit (lateral and vertical dimensions not to scale). Solvent evaporation is slower and solvent diffusion within the coating solution keeps composition more homogeneous. In this case, slight thickness differences impose different drying rates, but again differences in composition and surface tension can lead to the Marangoni effect.

References

1. Daniels, B.K., C.R. Szmanda, M.K. Templeton and P. Trefonas III. *Surface tension effects in microlithography - striations*. in *Advances in Resist Technology and Processing III*. 1986. SPIE v.631.
2. Rehg, T.J. and B.G. Higgins, *Spin Coating of Colloidal Suspensions.* AICHE Journal, 1992. **38**(4): p. 489-501.
3. Du, X.M., X. Orignac and R.M. Almeida, *Striation-Free, Spin-Coated Sol-Gel Optical Films.* Journal of the American Ceramic Society, 1995. **78**(8): p. 2254-2256.
4. Kozuka, H. and M. Hirano, *Radiative striations and surface roughness of alkoxide-derived spin coating films.* Journal of Sol-Gel Science and Technology, 2000. **19**(1-3): p. 501-504.
5. Kozuka, H., S. Takenaka and S. Kimura, *Nanoscale radiative striations of sol-gel-derived spin-coating films.* Scripta Materialia, 2001. **44**(8-9): p. 1807-1811.
6. Haas, D.E., D.P. Birnie, M.J. Zecchino and J.T. Figueroa, *The effect of radial position and spin speed on striation spacing in spin on glass coatings.* Journal of Materials Science Letters, 2001. **20**(19): p. 1763-1766.
7. Haas, D.E. and D.P. Birnie, *Nondestructive measurement of striation defect spacing using laser diffraction.* Journal of Materials Research, 2001. **16**(12): p. 3355-3360.
8. Haas, D.E. and D.P. Birnie. *Real-Time Monitoring of Striation Development During Spin-On-Glass Deposition*. in *Sol-Gel Commercialization and Applications (Ceramic Transactions, Vol 123, pp 133-138)*. 2001. American Ceramic Society.
9. Birnie, D.P., *Rational solvent selection strategies to combat striation formation during spin coating of thin films.* Journal of Materials Research, 2001. **16**(4): p. 1145-1154.
10. Haas, D.E. and D.P. Birnie, *Evaluation of thermocapillary driving forces in the development of striations during the spin coating process.* Journal of Materials Science, 2002. **37**(10): p. 2109-2116.
11. Taylor, D.J. and D.P. Birnie, *A case study in striation prevention by targeted formulation adjustment: Aluminum titanate sol-gel coatings.* Chemistry of Materials, 2002. **14**(4): p. 1488-1492.
12. Kozuka, H., *On ceramic thin film formation from gels: Evolution of stress, cracks and radiative striations.* Journal of the Ceramic Society of Japan, 2003. **111**(9): p. 624-632.
13. Kozuka, H., Y. Ishikawa and N. Ashibe, *Radiative striations of spin-coating films: Surface roughness measurement and in-situ observation.* Journal of Sol-Gel Science and Technology, 2004. **31**(1-3): p. 245-248.
14. Skrobis, K.J., D.D. Denton and A.V. Skrobis, *Effect of early solvent evaporation on the mechanism of the spin-coating of polymeric solutions.* Polymer Engineering and Science, 1990. **30**(3): p. 193-196.
15. Muller-Buschbaum, P., J.S. Gutmann, M. Wolkenhauer, J. Kraus, M. Stamm, D. Smilgies and W. Petry, *Solvent-induced surface morphology of thin polymer films.* Macromolecules, 2001. **34**(5): p. 1369-1375.
16. Strawhecker, K.E., S.K. Kumar, J.F. Douglas and A. Karim, *The critical role of solvent evaporation on the roughness of spin-cast polymer films.* Macromolecules, 2001. **34**(14): p. 4669-4672.
17. Luo, S.C., V. Craciun and E.P. Douglas, *Instabilities during the formation of electroactive polymer thin films.* Langmuir, 2005. **21**(7): p. 2881-2886.
18. Dario, A.F., H.B. Macia and D.F.S. Petri, *Nanostructures on spin-coated polymer films controlled by solvent composition and polymer molecular weight.* Thin Solid Films, 2012. **524**: p. 185-190.
19. Spangler, L.L., J.M. Torkelson and J.S. Royal, *Influence of solvent and molecular-weight on thickness and surface-topography of spin-coated polymer-films.* Polymer Engineering and Science, 1990. **30**(11): p. 644-653.
20. Scriven, L.E. and C.V. Sternling, *The Marangoni effects.* Nature, 1960. **187**: p. 186-188.
21. Benard, H., *Les tourbillons cellulaires dans une nappe liquide transportant de la chaleur par convection en regime permanent.* Annales de Chimie et de Physique, 1901. **23**: p. 62-144.
22. Rayleigh, L., *On convection currents in a horizontal layer of fluid, when the higher temperature is on the under side.* Philosophical Magazine (Series 6), 1916. **32**(192): p. 529-546.
23. Jeffreys, H., *The stability of a layer of fluid heated below.* Philosophical Magazine (Series 7), 1926. **2**: p. 833-844.
24. Block, M.J., *Surface tension as the cause of Benard cells and surface deformation of a liquid film.* Nature, 1956. **178**: p. 650-651.
25. Koschmieder, E.L. and M.I. Biggerstaff, *Onset of surface-tension-driven Benard convection.* Journal of Fluid Mechanics, 1986. **167**: p. 49-64.

26. Benguria, R.D. and M.C. Depassier, *On the linear-stability theory of Benard-Marangoni convection.* Physics of Fluids a-Fluid Dynamics, 1989. **1**(7): p. 1123-1127.
27. Buyevich, Y.A., L.M. Rabinovich and A.V. Vyazmin, *Chemo-Marangoni convection .1. Linear-analysis and criteria of instability.* Journal of Colloid and Interface Science, 1993. **157**(1): p. 202-210.
28. Stange, T.G., D.F. Evans and W.A. Hendrickson, *Nucleation and growth of defects leading to dewetting of thin polymer films.* Langmuir, 1997. **13**(16): p. 4459-4465.
29. Sehgal, A., V. Ferreiro, J.F. Douglas, E.J. Amis and A. Karim, *Pattern-directed dewetting of ultrathin polymer films.* Langmuir, 2002. **18**(18): p. 7041-7048.
30. Ashley, K.M., D. Raghavan, J.F. Douglas and A. Karim, *Wetting-dewetting transition line in thin polymer films.* Langmuir, 2005. **21**(21): p. 9518-9523.
31. Patton, T.C., *Paint Flow and Pigment Dispersion - A Rheological approach to coating and ink technology*. 1979: John Wiley and Sons.
32. Schwartz, L.W., D.E. Weidner and R.R. Eley, *An Analysis of the Effect of Surfactant on the Leveling Behavior of a Thin Liquid Coating Layer*. Langmuir, 1995. **11**(10): p. 3690-3693.
33. Joos, F.M., *Leveling of a film with stratified viscosity and insoluble surfactant.* AICHE Journal, 1996. **42**(3): p. 623-637.
34. Ma, H.M., R. Dong, J.D. Van Horn and J.C. Hao, *Spontaneous formation of radially aligned microchannels.* Chemical Communications, 2011. **47**(7): p. 2047-2049.
35. Bartlett, A.P., M. Pichumani, M. Giuliani, W. Gonzalez-Vinas and A. Yethiraj, *Modified Spin-coating Technique to Achieve Directional Colloidal Crystallization.* Langmuir, 2012. **28**(6): p. 3067-3070.
36. Uchiyama, H., Y. Mantani and H. Kozuka, *Spontaneous Formation of Linearly Arranged Microcraters on Sol-Gel-Derived Silica-Poly(vinylpyrrolidone) Hybrid Films Induced by Benard-Marangoni Convection.* Langmuir, 2012. **28**(27): p. 10177-10182.
37. Vanhook, S.J., M.F. Schatz, J.B. Swift, W.D. McCormick and H.L. Swinney, *Long-wavelength surface-tension-driven Benard convection: experiment and theory.* Journal of Fluid Mechanics, 1997. **345**: p. 45-78.
38. Oron, A., S.H. Davis and S.G. Bankoff, *Long-scale evolution of thin liquid films.* Reviews of Modern Physics, 1997. **69**(3): p. 931-980.
39. Yiantsios, S.G. and B.G. Higgins, *Marangoni flows during drying of colloidal films.* Physics of Fluids, 2006. **18**(8).
40. Bassou, N. and Y. Rharbi, *Role of Benard-Marangoni Instabilities during Solvent Evaporation in Polymer Surface Corrugations.* Langmuir, 2009. **25**(1): p. 624-632.
41. Yiantsios, S.G. and B.G. Higgins, *A mechanism of Marangoni instability in evaporating thin liquid films due to soluble surfactant.* Physics of Fluids, 2010. **22**(2).
42. Serpetsi, S.K. and S.G. Yiantsios, *Stability characteristics of solutocapillary Marangoni motion in evaporating thin films.* Physics of Fluids, 2012. **24**(12).
43. Haas, D.E., J.N. Quijada, S.J. Picone and D.P. Birnie. *Effect of Solvent Evaporation Rate on "Skin" Formation During Spin Coating of Complex Solutions*. in *Sol-Gel Optics V (pp280-284)*. 2000. SPIE3943.
44. de Gennes, P.G., *Solvent evaporation of spin cast films: "crust" effects.* European Physical Journal E, 2002. **7**(1): p. 31-34.
45. Birnie, D.P., *Surface skin development and rupture during sol-gel spin-coating.* Journal of Sol-Gel Science and Technology, 2004. **31**(1-3): p. 225-228.
46. Okuzono, T., K. Ozawa and M. Doi, *Simple model of skin formation caused by solvent evaporation in polymer solutions.* Physical Review Letters, 2006. **97**(13).
47. Birnie, D.P., D.M. Kaz and D.J. Taylor, *Surface tension evolution during early stages of drying of sol-gel coatings.* Journal of Sol-Gel Science and Technology, 2009. **49**(2): p. 233-237.
48. Sherman, F.S., *Viscous Flow*. McGraw-Hill Series in Mechanical Engineering. 1990: McGraw-Hill.
49. Meyerhofer, D., *Characteristics of resist films produced by spinning.* Journal of Applied Physics, 1978. **49**(7): p. 3993-3997.
50. Emslie, A.G., F.T. Bonner and L.G. Peck, *Flow of a viscous liquid on a rotating disk.* Journal of Applied Physics, 1958. **29**: p. 858-862.
51. Cobb, E.C. and O.A. Saunders, *Heat transfer from a rotating disk.* Proceedings of the Royal Society of London, Ser. A, 1956. **236**: p. 343-351.
52. Kreith, F., J.H. Taylor and J.P. Chong, *Heat and mass transfer from a rotating disk.* Journal of Heat Transfer, 1959. **81**(May): p. 95-105.

53. Sparrow, E.M. and J.L. Gregg, *Heat transfer from a rotating disc to fluids at any Prandtl number.* Journal of Heat Transfer, 1959. **81**: p. 249-251.
54. Horowitz, F., E.M. Yeatman, E.J.C. Dawnay and A. Fardad, *Real-time optical monitoring of spin coating.* Journal de Physique III, France, 1993. **3**: p. 2059-2063.
55. Horowitz, F., E.M. Yeatman, E.J.C. Dawnay and A. Fardad. *Optical monitoring of the sol to gel transition in spinning silica films*. in *Sol-Gel Optics III*. 1994. SPIE v.2288.
56. Gu, J., M.D. Bullwinkel and G.A. Campbell, *Solvent concentration measurement for spin-coating.* Journal of Applied Polymer Science, 1995. **57**(6): p. 717-725.
57. Birnie, D.P. and M. Manley, *Combined flow and evaporation of fluid on a spinning disk.* Physics of Fluids, 1997. **9**(4): p. 870-875.
58. Welty, J., C.E. Wicks, G.L. Rorrer and R.E. Wilson, *Fundamentals of Momentum, Heat and Mass Transfer*. 5th. ed. 2007, New York: John Wiley and Sons. 740.
59. Li, J.C.M. and P. Chang, *Self-diffusion coefficient and viscosity of liquids.* Journal of Chemical Physics, 1955. **23**: p. 518-520.
60. Suarez-Iglesias, O., I. Medina, C. Pizarro and J.L. Bueno, *On predicting self-diffusion coefficients from viscosity in gases and liquids.* Chemical Engineering Science, 2007. **62**(23): p. 6499-6515.